ESTIMATING ANNUAL SYNCHRONIZED 1-MIN POWER OUTPUT PROFILES FROM UTILITY-SCALE PV PLANTS AT 10 LOCATIONS IN NEVADA FOR A SOLAR GRID INTEGRATION STUDY

Joshua S. Stein[1], Clifford W. Hansen[1], Abraham Ellis[1], and V. Chadliev[2]
[1]Sandia National Laboratories, Albuquerque NM USA
[2]NV Energy, Las Vegas NV USA

ABSTRACT: We present an approach to simulate time-synchronized, one-minute power output from large photovoltaic (PV) generation plants in locations where only hourly irradiance estimates are available from satellite sources. The approach uses one-minute irradiance measurements from ground sensors in a climatically and geographically similar area. Irradiance is translated to power using the Sandia Array Performance Model. Power output profiles generated for 2007 in southern Nevada are being used for a Solar PV Grid Integration Study to estimate the integration costs associated with various utility-scale PV generation levels. Plant designs considered include both fixed-tilt thin-film, and single-axis-tracked polycrystalline Si systems ranging in size from 5 to 300 MW_{AC}. Simulated power output profiles at one-minute intervals were generated for five scenarios defined by total PV capacity (149.5 MW, 222 WM, 292 MW, 492 MW, and 892 MW) each comprising as many as 10 geographically separated PV plants.
Keywords: Grid Integration, Large Grid-connected PV systems, Simulation, Performance, Utilities

1 INTRODUCTION

NV Energy provides electricity to 2.4 million electric citizens throughout Nevada as well as a state tourist population exceeding 40 million annually. NVEnergy service area covers 45,592 square miles of the fastest growing state in the U.S.

In July 2010 the Public Utility Commission of Nevada requested that NV Energy study how different levels of photovoltaic (PV) generation would affect load balancing for the utility [1]. Sandia National Laboratories (SNL) participated in this study by producing time-synchronized, one-minute PV output profiles for proposed PV plants at 10 locations across southern Nevada (Figure 1). Five scenarios were considered, varying in the number of plants and the size of each plant, and ranging from 149.5 MW_{AC} up to 892 MW_{AC} total PV capacity. The scenarios and their constituent hypothetical PV plants are summarized in Table I.

Simulations were performed using satellite estimates and ground measurements of irradiance, as well as temperature and wind speed recordings for 2007; this year was selected for the study period because of the availability of data and because NV Energy recorded its highest peak load during that summer. NV Energy and its consultant, Navigant Consulting, used these profiles to calculate the effect on balancing operations (e.g., additional load following and regulation reserves) of various levels of utility-scale PV generation. NV Energy's study and findings are reported in Navigant, 2011 [2].

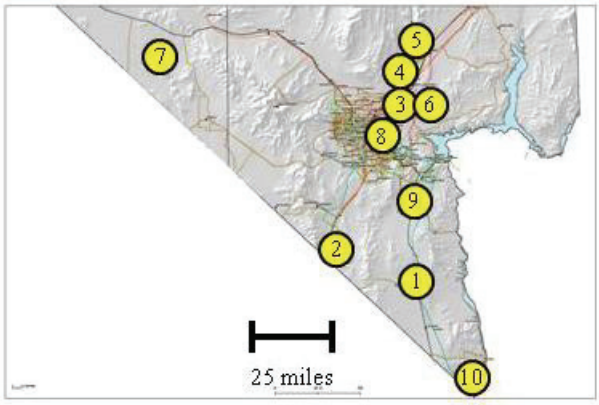

Figure 1. Map showing locations in southern Nevada for hypothetical PV plants considered in the study.

Table I. PV Plant Sizes (MW_{AC}) for each Scenario

	Scenario				
Site	**S1**	**S2**	**S3**	**S4**	**S5**
1	17.5	20	20	20	20
2*	50	50	100	100	300
3*	12	27	27	27	27
4	40	40	60	60	60
5*	-	50	50	100	200
6	30	30	30	30	30
7	-	-	-	50	100
8*	-	5	5	5	5
9*	-	-	-	50	100
10	-	-	-	50	50
Scenario Total (MW_{AC})	149.5	222	292	492	892

* These PV plants are specified to be latitude tilt, thin-film modules. Other plants are specified to be single axis tracking, polycrystalline Si modules

Here we document our method for simulating one-minute time series of power for each of the utility-scale

plants listed in Table I. We describe our simulation method in Section 2; results are summarized in Section 3.

In addition, the grid integration study required one-minute time series of aggregate power from small commercial (i.e., less than $3MW_{AC}$) and residential PV systems distributed throughout the Las Vegas valley. We estimated these time series using a simplified version of our simulation approach, which is summarized in [3] but not covered here.

2 METHODOLOGY

The instantaneous power output from a PV plant is determined by a number of factors, including: module and inverter characteristics; irradiance over the plant area; temperature of the PV cells; angle of incidence and spectral quality of the light; and losses, including soiling, wiring, and conversion losses.

Based on many years of outdoor module and array testing, Sandia has developed the Sandia PV Array Performance Model [4], which estimates instantaneous direct current (DC) power output from a PV module, given irradiance, angle of incidence, absolute air mass (i.e., the optical path length through the atmosphere, relative to solar zenith at sea level), ambient air temperature and wind speed. One challenge of applying this and other PV performance models to large PV systems is that the models generally expect a single value of irradiance as input. As PV systems become larger it is more likely that irradiance will vary spatially over the plant as cloud shadows pass over parts of the plant's footprint.

Studies performed by Sandia at the La Ola 1.2 MW PV plant in Lanai, HI [5] have illustrated the relationship between plant output and irradiance measured by a network of irradiance sensors spread over the plant footprint. The study results show that short-term (i.e., one-second) power output from a PV plant is approximately proportional to the spatial average of plane-of-array (POA) irradiance over the plant footprint. Figure 2 shows a scatterplot of one-second AC power from the plant against POA irradiance from a single sensor (red dots) within the plant and the spatial average of POA irradiance (blue dots) determined from 16 sensors distributed within the plant area. Scatterplots between power and POA irradiance measured at other single sensors are similar to the red dots in figure 2. The heavy black line indicates AC power as a function of irradiance that was measured during a clear day with steady irradiance. Excursions of the single sensor data (red dots) from the black line indicate periods of time when POA irradiance at the single sensor differed substantially from the spatial average irradiance over the plant area, due to the presence of cloud shadows over part, but not all, of the plant's area.

It is apparent from figure 2 that power output is better correlated with the spatial average of POA irradiance than with irradiance from a single sensor. The correlation between the spatial average of POA irradiance and power is observed across the range of irradiance and thus holds for both clear and cloudy conditions, implying that the spatial average of POA irradiance can be used in the PV performance model to predict power for all conditions.

Accordingly, our method broadly focuses on estimating one-minute spatial average of POA irradiance at the locations of each hypothetical PV plant, consistent with available information about irradiance at those locations. The spatial average of POA irradiance is then used in the Sandia PV Array Performance Model to estimate power from each plant.

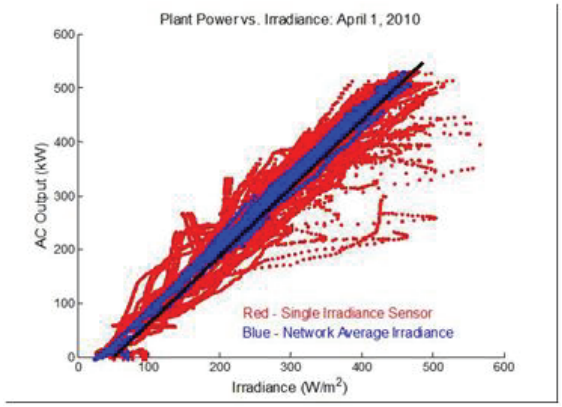

Figure 2. Relationship between irradiance and AC power from the entire La Ola plant for April 1, 2010, a partly cloudy day.

The method is outlined below as a sequence of steps:

1. Estimating one-minute global horizontal irradiance at a point at each study site;
2. Estimating spatially-averaged global horizontal irradiance over the footprint of each hypothetical PV plant;
3. Translating spatially-averaged global horizontal irradiance to spatially-averaged POA irradiance;
4. Calculation of one-minute AC power output.

2.1 Estimation of One-Minute Point Irradiance

Estimation of one-minute point irradiance involved downscaling (in time) from hourly information to one-minute time series. We discuss here: available data; review of published downscaling methods that have been applied to irradiance; and our selected approach.

2.1.1 Available Irradiance Data

No ground measurements of irradiance were available at any of the locations of the hypothetical PV plants during 2007. However, one-minute averages of global horizontal irradiance were available from pyranometers at other locations, namely, six Las Vegas Valley Water District (LVVWD) installations within the Las Vegas valley for the periods of time listed in Table II.

Table II. Irradiance Data Available from LVVWD Ground Measurements.

Station Name	Location	Start Date for Data	End Date for Data
Fort Apache	36.22N 115.30W	8/23/2006	4/29/2009
Grand Canyon	36.22N 115.31W	9/30/2006	4/29/2009
Las Vegas State Park	36.17N 115.19W	7/26/2007	4/29/2009
Spring Mountain	36.12N 115.29W	11/30/2006	4/29/2009
Luce	36.20N 115.26W	5/2/2007	4/29/2009

Ronzone	36.19N 115.23W	4/27/2006	4/29/2009

Estimates of irradiance at hourly intervals on a 10×10 km grid for the entire United States are available through the SolarAnywhere service from Clean Power Research [6]. This data is currently provided free of charge for time periods older than 3 years. Irradiance is estimated from GOES satellite imagery using algorithms developed by Perez and others [7]. These algorithms have been validated by several researchers [8-10]. Irradiance estimates at hourly intervals for the 10 study sites were obtained. These estimates represent instantaneous irradiance over a single satellite pixel (~1 km^2), which is somewhere in the 10×10 km area. Variability in the geopositioning of individual pixels can be as great as several kilometers between images. Lacking any other information about irradiance at each site, we regarded the satellite-derived irradiance values as instantaneous estimates of irradiance at each site. The satellite-derived irradiance values were used to calculate hourly averages of irradiance by averaging the two measurements which span the hour (the start and end of the hour).

2.1.2 Review of Downscaling Methods

To downscale from hourly average irradiance to one-minute irradiance at each site, we considered several options. We first reviewed a number of irradiance simulation models which aim to simulate time series of irradiance. These models generally simulate time-series of clearness index, i.e., irradiance divided by clear sky irradiance. Histograms of clearness index values are generally bimodal when the time intervals are short (e.g., one-minute), reflecting clear and cloudy conditions.

An approach suggested by Glasbey [11] involves simulating clearness index as a nonlinear autoregressive time series with the joint distributions of clearness at lag one defined by multivariate Gaussian mixtures. Components of the mixture are interpreted as representing different cloud conditions: clear skies; intermittent cloudy skies; and overcast conditions. Glasbey reports fitting the model to data from northeast Scotland and showed that simulated time-series reasonably reproduced the histogram of clearness index over time, and scatterplots of clearness index vs. lagged clearness index. We fit the proposed model form to one-minute irradiance data from LVVWD and used the fitted model to simulate time series of one-minute irradiance. We found that the variance in the simulated irradiance was generally higher than observed in the ground-based irradiance measurements. We attribute the higher variance to the low lag (i.e., one minute) considered in the fitted models, which appears to be too low to reproduce longer-period features evident in the LVVWD time series. In particular, the LVVWD data show many clear hours, interrupted by relatively infrequent periods of variable irradiance, and occasionally, by longer periods (i.e., several hours) of overcast conditions. The low lag causes the simulations to switch between mixture components too frequently to reproduce these features. Using the fitted model to produce time series of irradiance for the NV Energy study would have resulted in more frequent and/or larger ramps in simulated power than are supported by available data. We did not consider modifying the model form to introduce higher order lags.

Skartveit and Olseth [12] proposed a method to simulate five-minute clearness index from hourly average values determined by data. For each hour, they construct a distribution of five-minute clearness index values, sample from this distribution for each five-minute interval, and permute the sampled values to obtain a time series with lag one autocorrelation approximately equal to a target value. Each hour's distribution of five-minute clearness index values is modeled as a mixture of two beta distributions, the parameters of which are derived from the hourly clearness index, an estimate of the standard deviation of five-minute clearness index within the hour, and by matching characteristics of a training sample comprising five-minute average irradiance data from Atlanta, GA, San Antonio, TX, and Geneva, Switzerland. The estimated intra-hour standard deviation is sampled from a Wiebull distribution, the parameters for which are given by empirical equations resulting from the training sample. The model is tested by comparing simulated time series against five-minute irradiance collected at Payerne, Switzerland, from which the target autocorrelation was also obtained. The authors present two sets of histograms of clearness index, one conditional on solar elevation angle and a second conditional on average hourly clearness index, to show that the model acceptably matches the target data.

We considered but did not pursue using the Skartveit and Olseth model because of the low lag order lag used to account for autocorrelations. We believe that, if this model form were fit to the LVVWD data, that the simulated time series would exhibit higher variability than observed in the data, for the same reasons that simulated time series obtained using the Glasbey model were too variable. We did not consider revising the Skartveit and Olseth method to introduce higher order temporal correlations.

Tovar and others [13-16] have identified relationships between the frequency distribution of clearness index and other quantities such as the air mass and hourly average irradiance but do not specify a method for simulating time series. Essentially, these publications document various distribution forms that model the histogram of clearness index, conditional on values for other quantities such as air mass. Results in these papers are conceptually similar to Skartveit and Olseth [12], who use a mixture of beta distributions to describe the frequency distribution conditional on hourly average clearness index, and to Glasbey [11], who effectively uses a mixture of Gaussian distributions. Without an adequate method to account for autocorrelations (of relatively high order) in the one-minute time series of clearness index, simulations using these distribution forms would likely prove too variable, as we found for simulations using Glasbey's model, and as we suspect would have resulted using the model of Skartveit and Olseth. Consequently, we did not pursue simulating time series using, in some manner, the distributions described by Tovar and others.

2.1.3 Selected Downscaling Approach

Instead of simulating time series of irradiance, we selected an approach that replays recorded irradiance in a manner that: 1) closely reproduces the frequency distribution of hourly average irradiance, as determined from satellite observations; 2) results in one-minute time series of irradiance with variability similar to that observed at the LVVWD sites; and 3) honors any spatial and/or seasonal patterns that might exist in the hourly

averages. Our method starts by assembling a library of more than 5,000 one-day sequences of irradiance at one-minute intervals using all available ground station data (Table II). We calculated the hourly average irradiance for each day in the library. Next, for each day at each of the 10 study sites, we calculated the sum of the squared differences (SSD) between the target irradiance (hourly averages from satellite data) and the hourly average of irradiance for each of the library days. We then sorted the library days and kept track of the 10 library days with the lowest SSD (best fit) for each day of 2007 and at each site.

The next step involved assigning a library irradiance day (comprising a time-series of one-minute irradiance) to each site for each day of the year. To prevent the same library day being assigned to more than one site on the same day of the year, we generated a random permutation of integers from 1 to 10 for each day of the year. The permutation determined the order in which we assigned library days to the sites. For example, if the first four integers were 4, 1, 9, 2, … for a particular day, we began at Site 4 and chose the library day with the lowest SSD for that site and day. Next we examined Site 1. If the library day chosen for Site 4 also had the lowest SSD for Site 1, we chose the library day for Site 1 that had the second lowest SSD. We considered the remaining sites in the order specified by that day's permutation until each site was assigned a library day. Then we proceeded to the next day of the year and repeated the procedure. The permutation process ensures that the selection algorithm does not produce one-minute irradiance that is perfectly correlated between two sites on the same day. Figure 3 shows an example of the satellite irradiance for a day and the one-minute irradiance day from the library that was chosen.

The ground-based measurements of irradiance used to assign irradiance days to each plant location represent point measurements rather than spatial averages. The next step is to estimate the spatial average irradiance over each plant footprint. For this study we considered five scenarios (149.5 MW, 222 WM, 292 MW, 492 MW, and 892 MW). Each of these scenarios was defined as a mix of PV plants of varying sizes at each of the 10 sites (Table I).

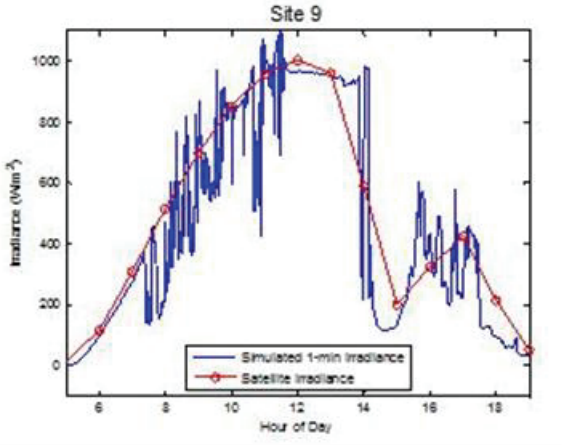

Figure 3. Comparison of satellite (red) and the best fit one-minute irradiance day.

2.3 Estimation of Spatially-Averaged Irradiance at Study Sites

Given a plant size (in MW_{AC}) and a technology (polycrystalline Si or thin-film), we made assumptions to estimate the total land area required (10 and 12.5 acres/MW_{AC} for Polycrystalline Si and Thin-film, repectively). For each plant listed in Table I, we calculated PV plant area as the product of the plant capacity (MW_{AC}) and the conversion factor (acres/MW_{AC}) for each plant type.

To estimate the spatial average irradiance over each plant, we applied the methodology developed by Longhetto et al. [17]. This method assumes that the spatial average of irradiance over an area can be estimated as a time average of point measurements of irradiance with an averaging window equal to the time it takes for a cloud to pass over the array. We estimated the characteristic length of the plant as the square root of the plant area (i.e., we assumed plants are square). The velocity of the cloud shadows across the landscape was estimated from upper air wind speed measurements made by NOAA from weather balloons launched from the Desert Rock station in Mercury, NV [18]. These balloons are launched every 12 hours throughout the year. We estimated wind speeds at cloud level as the average of the wind speeds measured from 1,000 to 8,000 meters above sea level. The mean upper air wind speeds for 2007 is 6.2 m/s (stdev = 3.4 m/s). We extended the twice-daily measurements into a one-minute time series by assuming that wind velocity was constant for five and one half hours after a measurement, then changed linearly over the succeeding hour to the next measured wind speed. Thus, wind speeds were constant for a total of eleven hours, and changed linearly over a period of one hour to the next constant value.

Effectively, the method for spatial averaging outlined above resulted in averaging windows (in time) most commonly between two and five minutes. Infrequently, averaging windows exceeded five minutes, and rarely were greater than ten minutes. Figure 4 illustrates the reduction in the variability of irradiance resulting from averaging over the plant area for three plants of increasing size. Greater reduction in variability is to be expected as plants become larger, due to the longer time required for cloud shadows to pass over the plant.

2.4 Translation to Plane-of-Array Irradiance

To apply the Sandia PV Array Performance Model [4] we need to calculate the direct and diffuse components of POA irradiance. We applied the DISC model [19] to estimate the direct normal irradiance (DNI) from global horizontal irradiance (GHI) and calculated the diffuse (horizontal) as the difference: GHI - DNI × cos(Z), where Z is the zenith angle. The DISC model is based on empirical data collected across the U.S. relating the diffuse fraction to GHI. Beam irradiance at the POA is DNI × cos(AOI), where AOI is the angle of incidence between the sun and the module surface. The AOI is calculated from Eq 1:

$$AOI = \cos^{-1}\begin{bmatrix}\cos(Z)\cos(T_a)+\\ \sin(Z)\sin(T_a\cos(A_s - A_a)\end{bmatrix} \qquad (1)$$

where Z is the solar zenith angle, T_a is the tilt angle of the array, A_s is the solar azimuth angle (0°=North, 90°= East), and A_a is the array azimuth angle (0°=North, 90°= East).

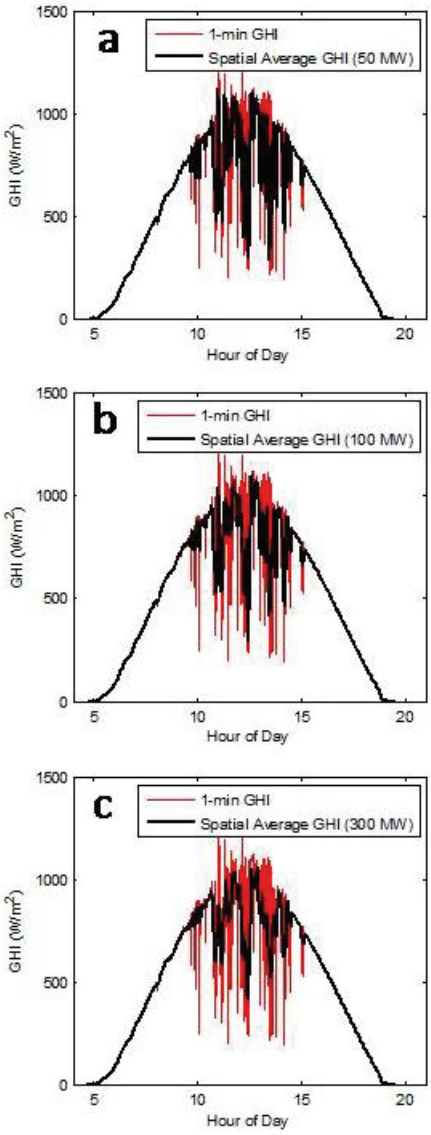

Figure 4. Comparison of one-minute point irradiance and estimated spatial average irradiance for three different plant sizes: 50 MW (a), 100 MW (b), and 300 MW (c).

In the case of the fixed (thin-film) arrays, *AOI* is simply a function of the solar zenith and azimuth angles, which vary with time. For single-axis tracked system (where the tracking axis is horizontal and oriented N-S), the tilt angle, array azimuth, and solar zenith angle vary with time. Eqs. 2 to 5 describe the calculation of the array tilt and azimuth angles, T_a and A_a for this configuration [20]:

$$\alpha = -\tan^{-1}\left[\frac{-\sin(Z)\sin(A_s)}{\cos(Z)}\right] \quad (2)$$

$$\beta = \left\{\begin{matrix} T_m \\ -T_m \\ \alpha \end{matrix}\right\} if \left\{\begin{matrix} \alpha > T_m \\ \alpha < -T_m \\ else \end{matrix}\right\} \quad (3)$$

where T_m is the maximum tilt angle for the tracker (assumed to be 45°).

$$T_a = |\beta| \quad (4)$$

$$A_a = \left\{\begin{matrix} 90° \\ 270° \end{matrix}\right\} if \left\{\begin{matrix} \beta >= 0 \\ \beta < 0 \end{matrix}\right\} \quad (5)$$

Diffuse irradiance on the POA was calculated using the translation model developed by Perez et al. [21]. The ground reflectance (albedo) was assumed to be constant (0.2). It is assumed that there is no shading of the arrays.

2.5 Calculation of One-Minute AC Power Output

DC power output from each array was estimated by using the Sandia PV Array Performance Model [4] to calculate the maximum power point for each minute of the year. AC power was determined from DC power by using the Sandia PV Inverter Model [22]. We assumed that the polycrystalline Si plants are constructed using Yingli Solar YL230-29b modules and that thin film plants use First Solar FS-275 modules; either module is representative of currently available technology. Both types of plants were assumed to be divided into 500 kW_{AC} blocks and use SatCon PVS-500 ($480V_{AC}$) inverters. Modules are assumed to be connected with a sufficient number of series strings so that the product of the assumed DC derate factor of 0.85 and the DC rating of the modules is equal to the AC rating of the system (in MW). These technology assumptions were necessary in order to run the models but are not likely to affect the model results in a significant way, because the differences in AC power output from similar modules and inverters are relatively small in comparison to the variability in power output due to the variability in irradiance.

Cell temperature was estimated using the King model [4], which accounts for the effects of POA irradiance, air temperature and surface wind speed. Air temperature and surface wind speed were derived from weather data recorded at McCarran International Airport in Las Vegas, NV. Measured surface wind speeds were used at each site without adjustment, while measured air temperature data was lapse-adjusted for elevation differences between each site and the airport meteorological station.

3. RESULTS AND CONCLUSIONS

The algorithm outlined in Section 2 was applied to generate one-minute time series of irradiance and power at each site contributing to each of the five scenarios summarized in Table I. Figure 5 shows an example of power output profiles from two days, one clear and one partly cloudy. A more extensive review of the results including a discussion of the validation of the simulation approach and results can be found in [3].

Figure 6 shows system net load (i.e. load – PV power) for different penetration levels on six representative days during the winter, spring and summer. Clear and partly cloudy days are shown to illustrate the impact of PV variability on net load (load – PV power). It is interesting to note that net load profiles indicate that PV generation in the winter and spring appear to reduce minimum system load which might affect baseload generation levels. Interhour net load variability appears to increase especially for high PV penetration scenarios.

NV Energy used these PV output profiles in a study to estimate integration costs associated with different levels of PV generation. The final study [2] was submitted to the Nevada Public Utilities Commission in July 2011 for its review.

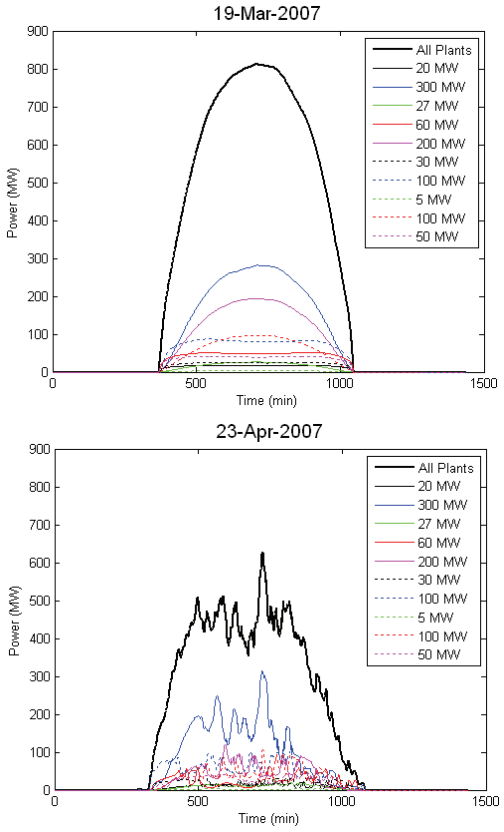

Figure 5. Power output profiles from two example days (top is a clear day and bottom is a partly cloudy day)

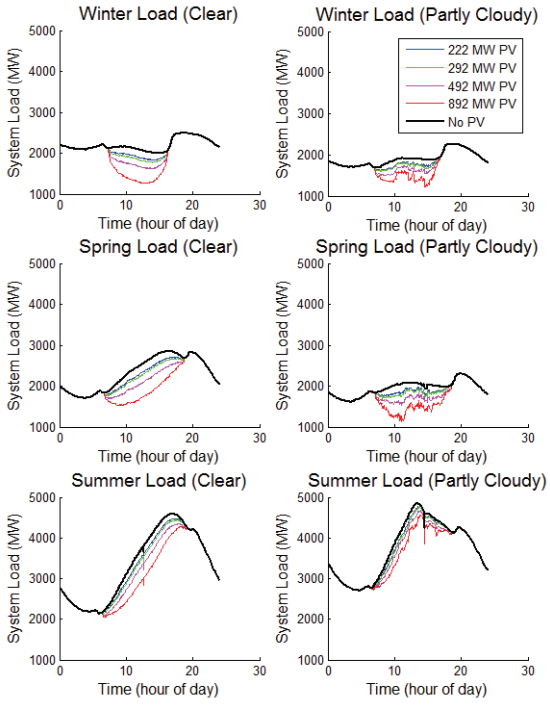

Figure 6. Six representative days of system net load with and without PV.

4. REFERENCES

1. Public Utility Commission of Nevada, Docket 10-02009, Granted Order dated 7/30/2010, Section W.
2. Navigant Consulting, Inc, *Large-Scale PV Integration Study*, Burlington, MA, July 30, 2011
3. Hansen, C.W., Stein, J.S, ,Ellis, A., SAND2011-5529, *Simulation of One-Minute Power Output from Utility-Scale Photovoltaic Generation Systems*, Sandia National Laboratories, Albuquerque, NM, 2011.
4. King, D. L., E. E. Boyson, et al., *Photovoltaic Array Performance Model*, SAND2004-3535, Albuquerque, NM, Sandia National Laboratories, 2004
5. Kuszmaul, S., A. Ellis, et al., *Lanai High-Density Irradiance Sensor Network for Characterizing Solar Resource Variability of MW-Scale PV System*, 35th IEEE PVSC, Honolulu, HI, 2010
6. Clean Power Research SolarAnywhere website: https://www.solaranywhere.com
7. Perez, R., Ineichen, P., Moore, K., Kmiecik, M., Chain, C., George, R., and Vignola, F, *A New Operational Satellite-to-Irradiance Model*, Solar Energy 73(5), pp.307-317, 2002
8. Stein, J., R. Perez, et al., *Validation of PV Performance Models using Satellite-Based Irradiance Measurements: A Case Study*. SOLAR2010, Phoenix, AZ, 2010
9. Perez, R., J. Schlemmer, et al., *Validation of the SUNY Satellite Model in a Meteosat Environment*. Proc., ASES Annual Conference, Buffalo, NY, 2009
10. Stackhouse, P., T. Zhang, et al., *Satellite Based Assessment of the NSRDB Site Irradiances and Time Series from NASA and SUNY/Albany Algorithms*, Proc. ASES Annual Meeting, San Diego, CA, 2008
11. Glasbey, C. A., *Nonlinear autoregressive time series with multivariate Gaussian mixtures as marginal distributions*, Applied Statistics 50: 143-154, 2001
12. Skartveit, A. and J. A. Olseth, *The probability density and autocorrelation of short-term global and beam irradiance*, Solar Energy 49(6) pp. 477-487, 1992
13. Tovar, J., F. J. Olmo, et al., *One-minute global Irradiance probability density distributions conditioned to the optical air mass*, Solar Energy 62(6): 387-393, 1998
14. Tovar, J., F. J. Olmo, et al., *One-minute k_b and k_d probability density distributions conditioned to the optical air mass*, Solar Energy 65(5), pp. 297-304, 1999
15. Tovar, J., F. J. Olmo, et al., *Dependence of one-minute global irradiance probability density distributions on hourly irradiation*, Energy 26, pp. 659-668, 2001
16. Tovar-Pescador, J., *Modelling the Statistical Properties of Solar, Radiation and Proposal of a Technique Based on Boltzmann Statistics*, in Modeling Solar Radiation at the Earth's Surface: Recent Advances, ed. V. Badescu. Berlin, Springer-Verlag, pp. 55-91, 2008

17. Longhetto, A., G. Elisei, et al., *Effect of correlations in time and spatial extent on performance of very large solar conversion systems*, Solar Energy 43(2), 77-84, 1989
18. Data obtained from University of Wyoming College of Engineering web service: http://weather.uwyo.edu/upperair/sounding.html Desert Rock station number is 72387.
19. Maxwell, E. L., *A Quasi-Physical Model for Converting Hourly Global Horizontal to Direct Normal Insolation*. Golden, CO, Solar Energy Research Institute, 1987
20. Chang, T. P., *The gain of single-axis tracked panel according to extraterrestrial radiation*, Applied Energy 86, pp. 1074-1079, 2009
21. Perez, Richard; Ineichen, Pierre; and Seals, Robert, *Modeling Daylight Availability and Irradiance Components from Direct and Global Irradiance*, Solar Energy 44(5), pp. 271-289, 1990
22. King, D. l., S. Gonzalez, et al., SAND2007-5036, *Performance Model for Grid-Connected Photovoltaic Inverters*, Sandia National Laboratories, Albuquerque, NM, 2007

5. ACKNOWLEGEMENTS

Sandia is a multiprogram laboratory operated by Sandia Corporation, a Lockheed Martin Company, for the United States Department of Energy's National Nuclear Security Administration under contract DE-AC04-94AL85000.